Clinical and Translational Science

ARTICLE OPEN ACCESS

Methods of Estimating Plasma Pharmacokinetics From Minimally Invasive, High Temporal Resolution Measurements of Interstitial Fluid Drug Concentrations

Murat K. Erdal[1] | Tod E. Kippin[2,3] | João P. Hespanha[1] | Kevin W. Plaxco[3,4,5]

[1]Department of Electrical and Computer Engineering, University of California, Santa Barbara, USA | [2]Department of Psychology and Brain Sciences, University of California, Santa Barbara, USA | [3]Biomolecular Science and Engineering Program, University of California, Santa Barbara, USA | [4]Department of Bioengineering, University of California, Santa Barbara, USA | [5]Department of Chemistry and Biochemistry, University of California, Santa Barbara, USA

Correspondence: Kevin W. Plaxco (kwp@ucsb.edu)

Received: 6 November 2024 | **Revised:** 3 March 2025 | **Accepted:** 28 April 2025

Funding: This work has been supported by NIH under the fund (EB022015).

Keywords: diffusion dynamics | electrochemical aptamer-based sensors | pharmacokinetics | therapeutic drug monitoring

ABSTRACT

In therapeutic drug monitoring, plasma drug concentrations are used to guide dosing decisions, significantly improving outcomes for many therapeutic interventions. Due to the cumbersome, laboratory-based approaches used to measure such drug concentrations, however, such monitoring is slow to return actionable information to the clinician and is performed far less frequently than would be optimal. In response, approaches are being developed by which in vivo drug concentrations can be monitored in real time and at high frequency in the subcutaneous or intradermal interstitial fluid—measurements that are safe, convenient, and minimally invasive. In the furtherance of this approach, here, we explore theoretically the ability to use such high-frequency sub- or intradermal measurements to estimate the corresponding plasma concentration–time courses, as the latter remain the basis of effectively all clinical decision making. Doing so, we find that, given various physiologically and technologically plausible assumptions, it is possible to accurately estimate plasma concentration–time courses from measurements of interstitial fluid taken at two nonredundant sites in the interstitial fluid. This ability to derive clinically important plasma pharmacokinetics using minimally invasive subcutaneous or intradermal sensor placements has the potential to significantly improve the precision and reach of therapeutic drug monitoring and, with that, the safety and efficacy of drug delivery.

1 | Introduction

Because it demonstrably improves safety and efficacy, therapeutic drug monitoring (TDM), the individualization of dosages to maintain in vivo drug concentrations within specified parameters, is a key element of the standard of care for many pharmacological therapies [1]. Unfortunately, however, current therapeutic monitoring approaches require blood draws and benchtop laboratory analysis, the cumbersome nature and slow "time-to-answer" of which have significantly limited the adoption of TDM [2]. Even when TDM is employed, it typically relies on only one or two measurements per drug administration [3–5]; such sparse sampling greatly reduces the precision with which the drug pharmacokinetics can be characterized, likely also reducing TDM's clinical value [4]. Against this background, recent advances in the real time, in vivo measurement of drug concentrations promise a potential revolution in such monitoring. Specifically, the ability of microns-diameter, millimeter-long electrochemical, aptamer-based (EAB) sensors to provide seconds-resolved, real-time

Summary

- What is the current knowledge on the topic?
  - Therapeutic drug monitoring (TDM) relies on plasma drug concentrations to guide dosing and thus enhance outcomes. However, due to their reliance on lab-based methods, plasma concentration measurements are infrequent and slow to return actionable results. Recent advances in high-frequency, real-time drug measurements in the subcutaneous or intradermal interstitial fluid (ISF) suggest a means of circumventing these issues, but at present, there is no predictive model for relating such measurements to the plasma drug concentrations on which clinical decision making is based Here, we explore this knowledge gap.
- What question did this study address?
  - How might high-precision, high-frequency drug concentration measurements performed in the ISF be used to accurately estimate plasma drug concentration–time courses, which remain central to clinical decision making?
- What does this study add to our knowledge?
  - The study demonstrates theoretically that, provided measurements are collected from two distinct subcutaneous or intradermal sites, plasma drug concentration profiles might be accurately estimated from ISF measurements. This approach leverages physiologically and technologically feasible assumptions to achieve precise plasma concentration estimations from less invasive monitoring techniques.
- How might this change clinical pharmacology or translational science?
  - By facilitating real-time therapeutic drug monitoring via minimally invasive subcutaneous or intradermal sensors, this method could significantly enhance dosing precision in clinical settings. As such, it offers a practical pathway to broaden TDM adoption, potentially increasing safety and efficacy in drug delivery and advancing personalized treatment strategies in clinical pharmacology.

measurements of free drug concentrations in situ in the living body [6–10] provides a route toward vastly improving the convenience and accuracy of TDM, and thus also its clinical impact.

Most of the subsecond-resolved, EAB-derived free drug measurements reported to date have been collected in plasma using intravenous sensors (e.g., [6, 11–14]), the invasiveness of which is less than ideal for day-to-day clinical use. That is, to achieve widespread applicability, it is likely that real-time drug measurements are best performed in the interstitial fluid (ISF) of the subcutaneous or intradermal space, a sample matrix that EAB sensors can access far less invasively and far more safely than plasma measurements [9, 10]; a strategy that has already been successfully applied to blood sugar with the continuous glucose monitor. To apply ISF-derived free drug concentration data to patient care, however, requires an ability to convert these measurements into clinically accurate estimates of the plasma free drug concentrations, which remain the basis of effectively all clinical decision making. Thus motivated, in this paper we theoretically explore scenarios in which highly time-resolved measurements of drug concentrations in the ISF might be used to accurately estimate plasma concentration–time profiles.

2 | Methods

The scenarios we explore in this work employ three assumptions. The first is that the drug in question is not eliminated from the body via local metabolism in the tissue compartment that is being observed. Given that we are considering observations in the subcutaneous or intradermal interstitial fluid (ISF), this assumption holds for most drugs, the majority of which are cleared hepatically or renally eliminated [15]. The second assumption is that the plasma and the ISF are the only relevant compartments (e.g., that the drug does not penetrate cells, or the ISF is in rapid equilibrium with intracellular fluids, rendering inter- and intracellular fluid a single compartment) and the free drug transfers between them only via passive diffusion (or, mathematically equivalently, via the bulk, pressure-driven flow of fluid into the tissues from the capillaries and out of tissue via the lymph system), an assumption that is commonly ascribed to (and found to hold reasonably well for) glucose [16, 17], and that likely holds for many drugs, including such important therapeutic drug-monitoring targets as the antibiotics vancomycin and the aminoglycosides, which are not metabolized in humans [18, 19]. The third assumption is that the rate constants describing molecular transport between the ISF and the plasma are, as their name implies, constant (we note that continuous glucose monitors have a "lock out period," presumably because tissues take time to "adjust" to the insertion of the device before the transport rate stabilizes). Under these assumptions, transport between the plasma and the ISF is described by,

$$\frac{dC_{ISF}(t)}{dt} = k_D\big(C_P(t) - C_{ISF}(t)\big), \tag{1}$$

where $C_{ISF}(t)$ and $C_P(t)$ are the time-dependent free drug concentrations in the ISF and plasma, respectively, and k_D is the rate constant for the target molecule's distribution between the two compartments [20].

While we also examine the case of measurements at a single site in the ISF (1), our main results consider measurements performed simultaneously at two, nonidentical sites. Hence, based on (1), we have the following pair of equations for which we will build our estimation methods.

$$\begin{aligned}\frac{dC_1(t)}{dt} &= k_1\big(C_P(t) - C_1(t)\big)\\ \frac{dC_2(t)}{dt} &= k_2\big(C_P(t) - C_2(t)\big),\end{aligned} \tag{2}$$

where $C_1(t)$ and $C_2(t)$ are the free drug concentration–time courses in the interstitial fluid at the two measurement sites, $C_P(t)$ is the plasma drug concentration–time course, and k_1, k_2 are the diffusion rate constants for drug transport between the plasma and the interstitial fluid at each of two sites. Our goal in

this work is to estimate the plasma concentration $C_P(t)$ based on the concentration measurements $C_1(t)$ and $C_2(t)$, which we do in two distinct ways.

2.1 | Known Pharmacokinetic Order

We start by studying the case when the structure of plasma pharmacokinetics is known. In particular, we assume that the drug pharmacokinetics in plasma follow a sum of exponential decays produced by a generic, stable, linear time-invariant system. We define this structure more rigorously as follows,

Definition 1. The plasma is said to exhibit n^{th} order pharmacokinetics if the concentration–time profile after a drug infusion can be expressed as a sum of n exponential decay terms of the form,

$$C_P(t) = \sum_{i=1}^{n} A_i e^{-k_{E_i} t}, \text{for all } t \geq 0, \tag{3}$$

where the k_{E_i} for $i = 1, 2, \dots, n$ are distinct rate constants associated with different pharmacokinetic processes (e.g., elimination, distribution into the tissues) and the A_i are relative weights of each process.

Remark 1. Equation (3) *represents the response to a particular infusion into the plasma, taking place before the start of observations (which occurs at time zero in* (3)*), that is, there are no additional drug infusions after time zero. Assuming that the underlying dynamics follow a linear, time-invariant compartmental model, meaning the pharmacokinetics is governed by constant diffusion rate constants* [20]*, this response also uniquely defines the input–output relation from a generic infusion to the drug concentration* [21]. In *other words, we can use the response given by* Equation (3) *to predict the drug concentration profile for any complex infusion profile. We state this observation formally as follows.*

Proposition 1. *Assume that the pharmacokinetic response is generated by a linear, time-invariant compartmental system and that the input drug infusion is constant over time intervals of length t_s. Then the input is defined by a time series of infusion rates, $u(0), u(t_s), \dots, u(Nt_s)$, and the output by a time series of plasma concentration values, $C_P(0), C_P(t_s), \dots, C_P(Nt_s)$, that satisfy the following relationship*:

$$C_P(kt_s) + \sum_{i=1}^{n} \alpha_i C_P((k-i)t_s) = \sum_{i=0}^{n-1} \beta_i u((k-i)t_s), \tag{4}$$

where the input is assumed to remain constant between the successive time points, and $C_P(t)$ stands for the n^{th} order plasma pharmacokinetics driven by the generic input, $u(t)$ (which is not necessarily zero after time $t = 0$). (For proof see Supporting Information).

In our first approach to estimating plasma pharmacokinetics from measurements performed in the ISF, we assume that the underlying pharmacokinetic order in the sense of ***Definition 1*** of the plasma concentration–time profile is known and, therefore, we have a difference equation of the form (4) in ***Proposition 1*** that defines the relation between the drug concentration in plasma at a given time and the details of the infusion history. We note that since our focus is to study the values of $C_P(t)$ at sampling times $t = 0, t_s, \dots, Nt_s$, it is convenient to convert the differential Equation (2) into a difference equation. To do that we need to make an assumption about how the $C_P(t)$ behaves between two sampling instances. Here, we use the simplest assumption and assume that it remains approximately constant, which is justified when the sampling time, t_s, is much smaller than the time constants associated with the pharmacokinetics in plasma; given the few-seconds resolution of EAB sensor measurements, this likely holds. This results in the following difference equations:

$$\begin{aligned} C_1((k+1)t_s) &= e^{-k_1 t_s} C_1(kt_s) + (1 - e^{k_1 t_s}) C_P(kt_s) \\ C_2((k+1)t_s) &= e^{-k_2 t_s} C_2(kt_s) + (1 - e^{k_2 t_s}) C_P(kt_s) \end{aligned} \tag{5}$$

where $C_1(t)$ and $C_2(t)$ stand for the concentration values at the first and second ISF measurement sites at time t. Further, we assume that the measurements of the ISF concentration–time profiles are "corrupted" by zero-mean Gaussian noise with variances σ_1^2, σ_2^2, respectively. We denote the two noisy ISF measurements by $y_1(kt_s)$ and $y_2(kt_s)$ for $k = 0, 1, \dots, N$ for the two sites such that,the system equations

$$\begin{aligned} y_1(kt_s) &= C_1(kt_s) + \varepsilon_1(k) \\ y_2(kt_s) &= C_2(kt_s) + \varepsilon_2(k) \end{aligned} \tag{6}$$

where $C_1(kt_s)$ and $C_2(kt_s)$ are the true concentration values at the measurement sites and the $\varepsilon_1(k)$ and $\varepsilon_2(k)$ are zero-mean Gaussian measurement noises at the k^{th} measurement. This allows us to formulate the log-likelihood of the observed measurements for given parameter values.

$$\begin{aligned} J(\{\alpha_i, \beta_{i-1}\}_{i=1}^{n}, k_1, k_2\sigma_1^2, \sigma_2^2) = &\sum_{j=1}^{2} \frac{N+1}{2} log\left(2\pi\sigma_j^2\right) \\ &- \frac{1}{2\sigma_j^2} \sum_{k=0}^{N} \left(y_j(kt_s) - C_j(kt_s)\right)^2 \end{aligned} \tag{7}$$

This formulation along with the system equations given in (5) allows us to cast the problem of estimating the parameter values $\theta = (\{\alpha_i, \beta_{i-1}\}_{i=1}^{n}, k_1, k_2\sigma_1^2, \sigma_2^2)$ as well as the plasma concentration $C_P(t)$ for $t = 0, t_s, \dots, Nt_s$ as the following maximum-likelihood optimization

$$\max_{\theta, C_1(t), C_2(t), C_P(t) \text{ for } t = 0, t_s, \dots, Nt_s} J(\theta) \tag{8}$$

where the maximization is taken over a set defined by the equality constraints (4) and (5), and the inequality constraints over $\{\alpha_i, \beta_{i-1}\}_{i=1}^{n}$ listed in ***Proposition S1***, as well as positivity constraints on the diffusion rates k_1, k_2, and the noise variances σ_1^2, σ_2^2.

If the pharmacokinetic order of the drug, n, is known (from the literature or from prior studies) we can use nonlinear programming tools [22, 23] to solve the problem (8) and infer the pharmacokinetics of the plasma. Alternatively, however, if the true pharmacokinetic order is unknown, we can solve the

problem (8) for a number of "candidate" pharmacokinetic orders and then use statistical tests to determine which is the most appropriate descriptor. For this we use the Bayesian information criterion (BIC) [24, 25],

$$BIC_n = n_p log(2N) + 2J\left(\hat{k}_1, \hat{k}_2, \left\{\hat{\alpha}_i, \hat{\beta}_{i-1}\right\}_{i=1}^{n}, \hat{\sigma}_1^2, \hat{\sigma}_2^2\right), \quad (9)$$

where $n_p = 2n + 4$ is the number of parameters estimated, $\hat{k}_1, \hat{k}_2, \left\{\hat{\alpha}_i, \hat{\beta}_{i-1}\right\}_{i=1}^{n}, \hat{\sigma}_1, \hat{\sigma}_2$ are the estimates of the model parameters, as introduced in (2), (5), (7) for an assumed model order n in plasma. This measure allows us to select the most appropriate model to explain the observed measurements $C_1(t), C_2(t)$.

2.2 | Minimum Assumptions Fit

In the above-described approaches, we assumed that plasma pharmacokinetics are well described as the sum of some number of exponentials after an intravenous drug infusion. We can also, however, estimate $C_P(t)$ from measurements of $C_1(t)$ and $C_2(t)$ without making any assumptions about the functional structure of the plasma pharmacokinetics. We start by noting that the equations describing the pharmacokinetics of dual ISF compartments (2) can be rearranged to have a familiar regression structure with the plasma concentrations $C_P(t)$ as part of the regression vector.

$$\begin{bmatrix} \overline{C_1} \\ \overline{C_2} \end{bmatrix} = \begin{bmatrix} -\overline{dC_1} & \bar{0} & I \\ \bar{0} & -\overline{dC_2} & I \end{bmatrix} \begin{bmatrix} 1/k_1 \\ 1/k_2 \\ \overline{C_p} \end{bmatrix}, \quad (10)$$

where $\overline{C_1}$, $\overline{C_2}$ and $\overline{C_P}$ are vectors of values $C_1(t), C_2(t)$, and $C_P(t)$ over the available time instants, $\overline{dC_1}$ and $\overline{dC_2}$ are vectors of values $\frac{dC_1(t)}{dt}$, $\frac{dC_2(t)}{dt}$, respectively, $\bar{0}$ is a vector of zeros and I is the identity matrix of appropriate sizes.

Equation (10) allows the estimation of the diffusion coefficients k_1, k_2 and the plasma concentration values $C_P(t)$ that appear in the right-hand side vector, based on the left-hand side vector and the matrix at the center. However, to form this matrix we need to compute derivatives of concentration–time profiles at the ISF measurement sites. To accomplish this, we use a second-order smoothing-spline approach to estimate the derivatives of $C_1(t)$ and $C_2(t)$. We selected a second order spline because the minimum required smoothness level that supports the continuous derivatives of the ISF concentration we require. We note that higher order splines would thus also work, but this would extend the minimum window of data employed, harming time resolution. To do this, we fit second order polynomials to the data as follows:

$$C_i(t) = a_{i,j}\left(t - T_j\right)^2 + b_{i,j}\left(t - T_j\right) + c_{i,j} \quad (11)$$

for $T_j \le t < T_{j+1}$, $j = 0, 1, \ldots, N_s$ and $i = 1, 2$, where $\left[T_j, T_{j+1}\right)$ are smoothing intervals over which the data will be smoothed by a polynomial fit, $\left(a_{i,j}, b_{i,j}, c_{i,j}\right)$ are the coefficients for such polynomials and N_s is the number of such intervals. We take the smoothing intervals to be of all equal length, corresponding to knot locations given by $T_j = jn_sT$, meaning that each smoothing interval will be of length n_sT. Then for a given interval length n_s, we define the cost function for our fit as

$$J_{n_s}(\theta) = \sum_{p=0}^{N-1} \sum_{i=1}^{2} \frac{N}{2} log\left(2\pi\sigma_i^2\right) + \frac{1}{2\sigma_i^2}\left(Y_i(pT) - C_i\left(pT; \theta_i\right)\right)^2, \quad (12)$$

where

$$C_i\left(pT; \theta_i\right) = a_{i,j}\left(p_jT\right)^2 + b_{i,j}\left(p_jT\right) + c_{i,j}, \text{for } i = 1, 2 \text{ and } j = 0, \ldots, N_s \quad (13)$$

subject to constraints

$$c_{i,j+1} = \left(n_sT\right)^2 a_{i,j} + \left(n_sT\right) b_{i,j} + c_{i,j} \quad (14)$$

$$b_{i,j+1} = \left(2n_sT\right) a_{i,j} + b_{i,j} \quad (15)$$

$$b_{i,j} = k_{D_i}\left(C_P\left(jn_sT\right) - c_{i,j}\right) \quad (16)$$

where θ is the collection of all parameters that affects the overall cost, σ_i^2 is the measurement noise variance and $\theta_i = \left(a_{i,j}, b_{i,j}, c_{i,j}\right)_{j=0}^{N_s}$ is the collection of $N_s + 1$ sets of polynomial coefficients for the i^{th} compartment, $p_j = p - jn_s$ is the difference between p and the largest integer that is smaller than p and divisible by n_s, and $Y_i(pT)$ is the noisy measurement from the i^{th} compartment at time instant pT, and $C_P\left(jn_sT\right)$ is the value of plasma concentration levels at time jn_sT, that is, once every n_sT periods. Here, we note that the smoothness constraints (14), (15), follow from the spline structure to make sure that the values of concentration, or their derivatives do not suddenly change every spline period, that is, every n_sT time intervals. We also note that the dynamics constraints (16) allows us to link two concentration–time profiles and they follow from the assumption on the dynamics we made earlier (2) with the spline structure given at (13).

3 | Results

3.1 | Estimating Plasma Pharmacokinetics From Single-Site ISF Measurements

The easiest method for estimating the plasma drug concentration–time course, $C_P(t)$, using concentration measurements performed in the ISF, $C_{ISF}(t)$, arises when (*i*) the assumption of passive diffusion (and the accompanying dynamics described by Equation (1)) holds and (*ii*) the timescale associated with diffusion between the plasma and the ISF($\sim 1/k_D$) is significantly shorter than the timescale of the most rapid, clinically relevant changes in plasma concentration. Specifically, as the difference between these timescales increases, the time course of the drug in the ISF approaches its time course in the plasma and thus the latter can be estimated by assuming it is equivalent to the former. Of note, due to glucose's low molecular weight (and thus its rapid diffusion into the tissues)

and the relatively small magnitude and slow timescale with which its plasma concentrations fluctuate (e.g., the concentration rise and fall after eating is typically less than 2-fold and occurs over many minutes), this scenario is a reasonable approximation for the relationship between its plasma and ISF concentrations, and thus continuous glucose monitors employ this assumption in their analysis [26]. To put this idea on a more quantitative footing, here, we have modeled a drug that exhibits first-order elimination kinetics,

$$C_P(t) = C_{max} e^{-k_E t}, \tag{17}$$

where k_E is the first order elimination rate constant and the C_{max} is the maximum plasma concentration seen after an instantaneous bolus drug injection at time $t = 0$. Under this scenario, we find that, even when the injection is assumed to be instantaneous (rendering the correspondence between the C_{max}^{plasma} in blood and ISF poorer than it would be were the drug infused slowly), if k_D is 10-fold greater than k_E, the plasma and ISF pharmacokinetics track one another rather closely (Figure 1A). Specifically, in this scenario the half-life observed in ISF is only 15% slower than the half-life seen in plasma (Figure 1B). Similarly, the maximum concentration reached in the ISF, C_{max}^{ISF}, is within about 20% of the plasma maximum, C_{max}^{plasma}, (Figure 1C). Note that this scenario is similar to the situation for glucose monitoring, as glucose, being a fairly small molecule, diffuses into the tissues rather rapidly relative to the timescale of its plasma fluctuations under any normal physiological scenario, that is, in the absence of rapid intravenous delivery of the sugar. As k_D approaches k_E, however, the accuracy of simply assuming that the plasma time course equals the ISF time course degrades. For example, when k_D is only 3-fold faster than k_E the half-life in ISF is about 50% longer than that seen in plasma and C_{max}^{ISF} falls approximately 40% short of C_{max}^{plasma}. And when k_D equals k_E, the half-life in ISF stretches to ~240% that of the plasma and C_{max}^{ISF} falls to only 1/3 of the C_{max}^{plasma}.

Under the assumptions we have employed, measurements performed in the ISF can also provide clinically important constraints on plasma pharmacokinetics in scenarios in which, in contrast to the scenario described above, the timescales of the most rapid changes in plasma concentration are similar to the timescales of distribution into the ISF. Specifically, while ISF drug time courses might not clearly define C_{max}^{plasma}, as long as Equation (1) holds, ISF-derived measurements can be used to determine plasma drug exposure (as the "area under the curve"; AUC_{plasma}). This is because, under the assumptions employed here, AUC_{plasma} asymptotically approaches the area under the curve observed in the ISF (AUC_{ISF}), and thus the latter can be used to estimate the former to any desired precision degree if one collects data for sufficiently long. We state this result more rigorously in the following theorem, the proof of which is provided in the Supporting Information.

Theorem 1. *Let $C_P(t)$ and $C_{ISF}(t)$ denote the drug concentration–time profiles in the plasma and the ISF, respectively, and define the respective areas under the curves (AUC) as*

$$AUC_{plasma} = \int_0^\infty C_P(t)dt, AUC_{ISF} = \int_0^\infty C_{ISF}(t)dt. \tag{18}$$

If AUC_{plasma} is finite, then, under the passive diffusion assumption (1) with $k_D > 0$, we have

$$AUC_{plasma} = AUC_{ISF}. \tag{19}$$

While Theorem 1 provides a means of estimating AUC_{plasma} from AUC_{ISF}, it does not provide a means of estimating the underlying plasma concentration–time profile, a result that would presumably be of still greater clinical value.

Even under the simplifying approximations we have invoked, a drug's plasma concentration–time course cannot be uniquely determined from measurement of its concentration at a single site in the ISF. To understand why this is true, consider a drug that obeys a simple two-compartment model where the drug pharmacokinetics in the plasma is dominated by a constant elimination rate, as assumed in (17), and the drug can only enter to and exit from the ISF through passive means from and to the

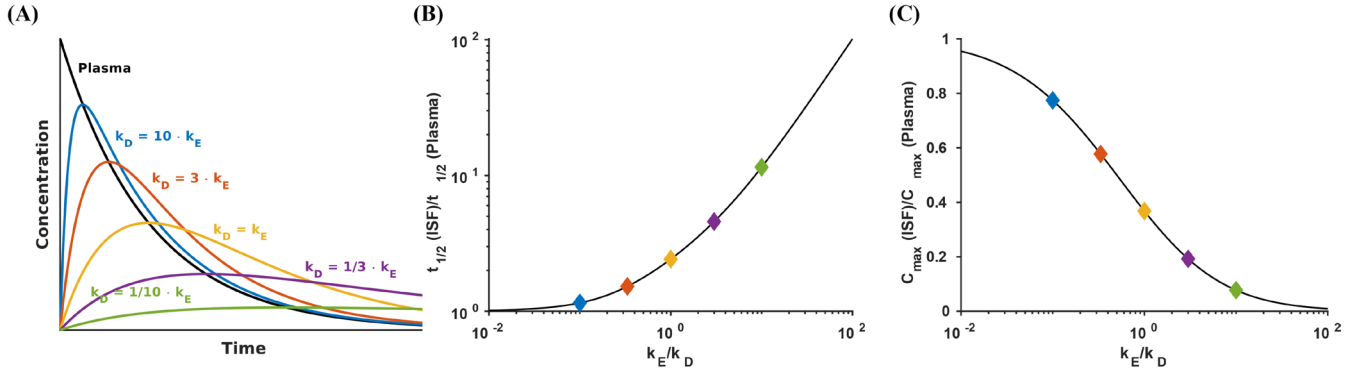

FIGURE 1 | (A) As long as (*i*) the rate constant for distribution between the plasma and the ISF, k_D, is at least a few-fold higher than the fastest rate of change in the plasma concentrations (here, the elimination rate from the blood, k_E)and (*ii*) the drug transport between ISF and the plasma is governed by passive diffusion (equation (1), then drug concentrations in plasma (black curve) reasonably approximate those seen in the ISF (colored curves). (B) As shown, for example, when the distribution rate constant is 10 times more rapid than the elimination rate constant the half-life (after the peak concentration is achieved) seen in the ISF is only about 15% slower than that seen in the plasma and (C) the peak concentration in ISF, C_{max}^{ISF} reaches 80% of C_{max}^{plasma}. The ratios considered in panel A are highlighted using the same colors in panel B and C.

plasma, as given in (1). Under these circumstances the drug's pharmacokinetics are described by:

$$\begin{aligned}\frac{dC_P(t)}{dt} &= -k_E C_P(t) + \frac{1}{V_P}u(t)\\ \frac{dC_{ISF}(t)}{dt} &= k_D\left(C_P(t) - C_{ISF}(t)\right)\end{aligned} \tag{20}$$

where k_E is the rate constant for elimination from the plasma, k_D is the rate constant for transport between the plasma and the ISF, V_P is the apparent distribution volume of the plasma, and $C_P(t)$ and $C_{ISF}(t)$ are the concentration–time courses in plasma and ISF, respectively. Even for this simplest case, which is described by only 3 unknown parameters (k_E, k_D and V_P), there are always two plasma time courses (differing in k_E and k_D) [27] that could produce the given ISF time course (see ***Proposition S2*** and Figure 2B), such that time courses collected at a single site in the ISF will always produce ambiguous estimates of the plasma time course. And the situation for models that include more than two compartments is still worse. For example, there are infinitely many plasma time courses consistent with a given ISF time course under a three-compartmental model (see ***Proposition S3*** and Figure 3A).

3.2 | Dual Measurement Sites

Provided that our assumptions hold (i.e., that equation (1) holds), a solution exists by which we can resolve the ambiguous estimates of

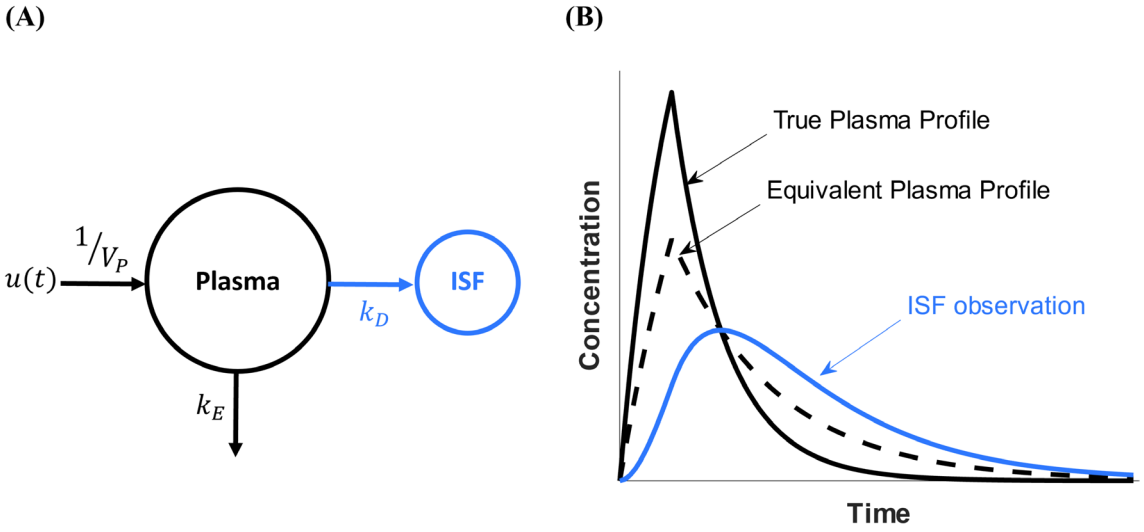

FIGURE 2 | Even under a simple, two-compartment model, observations in the secondary compartment (here, ISF) do not provide enough information to unambiguously predict the concentrations in the central compartment (here, plasma) (A) This simple model includes drug delivery into the plasma followed by transport into the ISF compartment with a distribution rate constant, k_D and elimination from the plasma via first-order kinetics with an elimination rate constant, k_E. (B) Even under this highly simplified model, there are two, distinctly different plasma concentration–time profiles that could produce any observed ISF concentration–time profile.

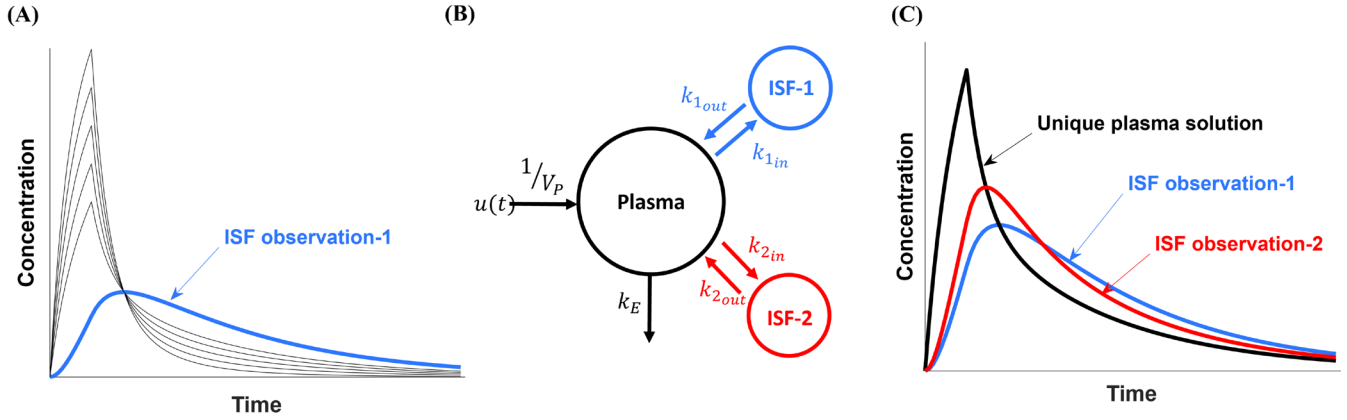

FIGURE 3 | (A) Due to a mathematical redundancy, observations collected at a single site in the ISF are unable to uniquely define the plasma concentration–time course that is generating them (see ***Proposition S2***), thus leading to infinitely many mathematically equivalent estimates of plasma concentration–time profiles. (B) Under the assumptions employed here, however, we can overcome this ambiguity by employing observations from a pair of nonredundant ISF measurement sites (red and blue) differing in the rate constants that describes drug transport between these sites and the plasma. (C) Such a pair of measurements can be used to derive a unique estimate of the plasma concentration–time profile.

plasma pharmacokinetics: the use of measurements performed at two, nonredundant sites in the ISF for which k_D differs by some degree. This scenario is described by equation (2). To state this observation more formally, we first define a concept of "unambiguity."

Definition 2. Consider a model with an output $y(t)$, such as model (2) with output $y(t)$ that may include only $C_1(t)$, only $C_2(t)$ or both $C_1(t)$ and $C_2(t)$. We say that the parameters defining the model, such as diffusion rates k_1, k_2 and plasma concentration profile $C_P(t)$, are uniquely identifiable if any two nonidentical sets of variable values corresponds to two distinct outputs.

Using the notion of unique identifiability, we can state the main result of this work as the following theorem.

Theorem 2. *Let $C_P(t)$ denote the drug concentration–time profile in the plasma. Assume that $C_1(t)$ and $C_2(t)$ denote two different ISF concentration–time profiles resulting from $C_P(t)$ under the simple diffusion dynamics of (2) with diffusion rate constants k_1 and k_2, respectively. If we assume zero concentrations $C_1(t) = C_2(t) = C_P(t) = 0$ before time $t = 0$,*

1. *k_1 and $C_P(t)$ are not uniquely identifiable by using only $C_1(t)$. Similarly, k_2 and $C_P(t)$ are not uniquely identifiable by using only with $C_2(t)$*
2. *k_1, k_2 and $C_P(t)$ are uniquely identifiable by using both $C_1(t)$ and $C_2(t)$ if $k_1 \neq k_2$.*

(For the proof, see Supporting Information)

Next, we explore the implications of this result, starting with a fairly constrained scenario before progressing to significantly less constrained scenarios.

We first demonstrate that the plasma concentration–time course can be uniquely estimated from dual, nonredundant ISF measurements in the simplifying case of having some *a priori* knowledge of the structure of the drug's plasma time course. Specifically, we assume that the plasma time course seen following a drug infusion can be described as the sum of a specific, known number, n, of exponential decays,

$$C_P(t) = \sum_{i=1}^{n} A_i e^{-k_{E_i} t}, \tag{21}$$

where A_i and k_{E_i} are the relative magnitude and the elimination rate constant, respectively, of the i^{th} exponential decay.

We call the number of exponential decay profiles appearing the pharmacokinetic order (see ***Definition*** 1), for example the simple example (17) is of pharmacokinetic order 1 (i.e., is a one-compartment model). We can then estimate the distribution coefficients, along with the parameters that define the plasma concentration–time profile, from the observed, noisy ISF measurements and the known intravenous drug infusion profile. To demonstrate this, we simulated systems in which (a) the plasma pharmacokinetics are of pharmacokinetic order 1, 2 or 3, (b) the signal-to-noise ratio (SNR) of the ISF measurements is 30 and the rate constants for distribution into the tissues at the two observation sites differ by some factor. The SNR value is consistent with recently reported subcutaneous measurements [9] and given the improvements in the EAB sensor platform, we only expect this ratio to be improved as the technology is optimized. In our first analysis, we assumed that the rate constants for distribution to the two ISF sites are $k_1 = 0.15$ min^{-1} and $k_2 = 0.075$ min^{-1}, that is, they differ by a factor of 2 to generate the data. Under these circumstances, the plasma drug time course and the distribution rate constants, k_1 and k_2, can be estimated from the paired ISF measurements uniquely and with excellent precision (Figure 4).

Although in the above study we employed a priori knowledge of the order of the plasma pharmacokinetics (Figure 4), the ability to estimate plasma concentration–time courses from time-resolved measurements at two ISF sites does not actually require such foreknowledge. One way to achieve accurate plasma estimates without foreknowledge of their structure is to perform fits to a set of candidate pharmacokinetic orders, and then use a selection criterion such as the Bayesian Information Criterion (BIC; see ***Methods*** for details) to determine the preferred model. BIC punishes the model complexity while rewarding the fit quality, which results in selecting the least complex model that still explains the data well [25]. To illustrate this approach, we generated realistically noisy ISF data driven by second-order compartmental plasma kinetics and then fit the resulting ISF data assuming first-, second-, or third-order compartmental models. The BIC values associated with the three models, 1169, 481, and 492 for first-, second-, and third-order models, respectively, correctly identified the second-order model (lowest BIC) as the appropriate model for the plasma pharmacokinetics (Figure 5).

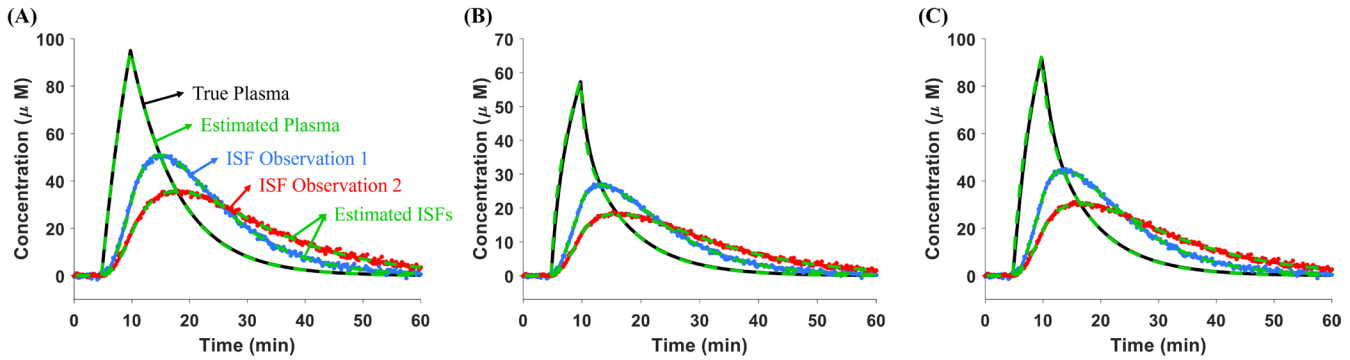

FIGURE 4 | Assuming we have foreknowledge of the appropriate pharmacokinetic model, a nonredundant pair of noisy ISF measurements (red and blue curves) can be used to estimate plasma concentration–time courses with high precision. Here, we have employed compartmental models of order 1, 2, and 3 in panels A, B, C, respectively. The fitted ISF profiles and the estimated plasma profiles are shown by dashed green lines, and the true plasma profiles as solid black line. Here, the distribution rate constants for the two nonredundant ISF sites differ by a factor of 2.

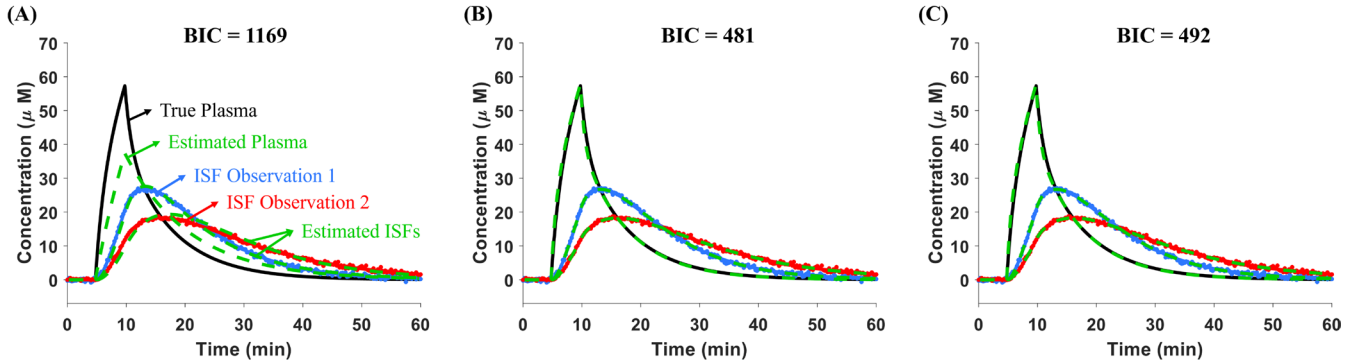

FIGURE 5 | Assuming the plasma concentration–time courses follows one of the pharmacokinetic models in an applied set of models, we can use the Bayesian Information Criterion (BIC) to select the plasma pharmacokinetic model most likely to explain an observed, nonredundant pair of ISF concentration–time profiles. (A–C) Here, the "true" plasma pharmacokinetics follow a second order compartmental model (Equation (5) with $n=2$ and where the noise–free true concentration–time profile in plasma is given by the black solid line and the fits are presented under the assumption of plasma pharmacokinetics follow compartmental models of order one (A), two (B) or three (C). The minimal value of BIC is associated with the second order model, thus correctly indicating that it is the most appropriate model.

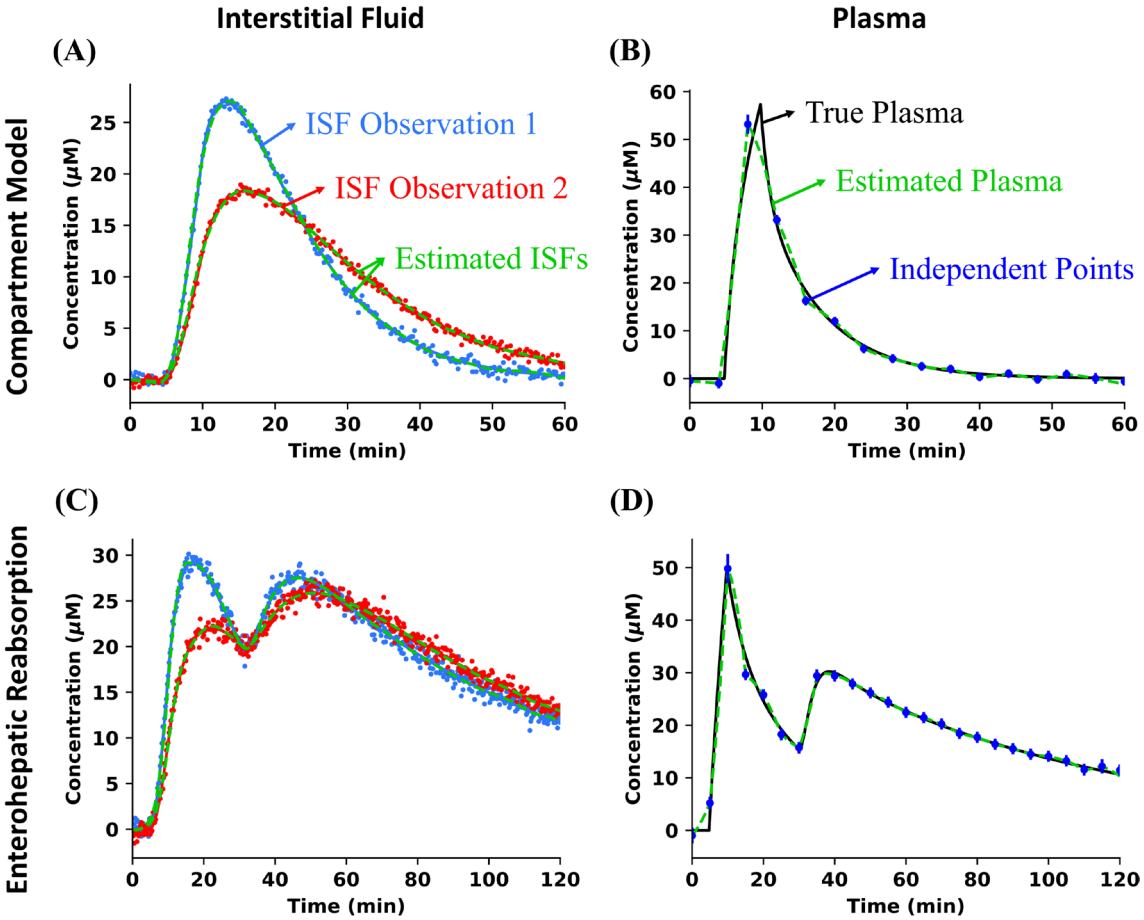

FIGURE 6 | Measurements collected at two nonredundant ISF sites are sufficient to accurately estimate the plasma concentration–time profile even in the absence of any foreknowledge of the structure of the plasma pharmacokinetics. To demonstrate this "Minimum Assumptions Fit" approach, here, we have employed two scenarios: One in which the plasma kinetics follow a single-compartment model (A, B), and another in which the plasma concentration exhibits the effect of enterohepatic reabsorption (EHR), a pharmacokinetic mechanism that can generate significantly non-monotonic plasma concentration–time courses [29] (C, D). We used these two plasma profiles (solid black lines in panels B and D) to generate pairs of corresponding ISF time courses (blue and red dots, panels A and C) to which we added simulated noise at typical experimental levels (signal-to-noise ratio = 30). Fitting the resulting noisy ISF profiles (green lines, panels A and C) returns estimates (blue dots, panels B and D) that mirror the true plasma drug profiles (black curves, panels B and D) to a clinically relevant degree of accuracy. Here (panels B and D), the 95% confidence intervals for our estimates are shown as solid blue lines. The estimated interpolated values in between freely estimated values are shown by the green dashed lines (B, D). For model and pharmacokinetic parameters, see Tables S1 and S2.

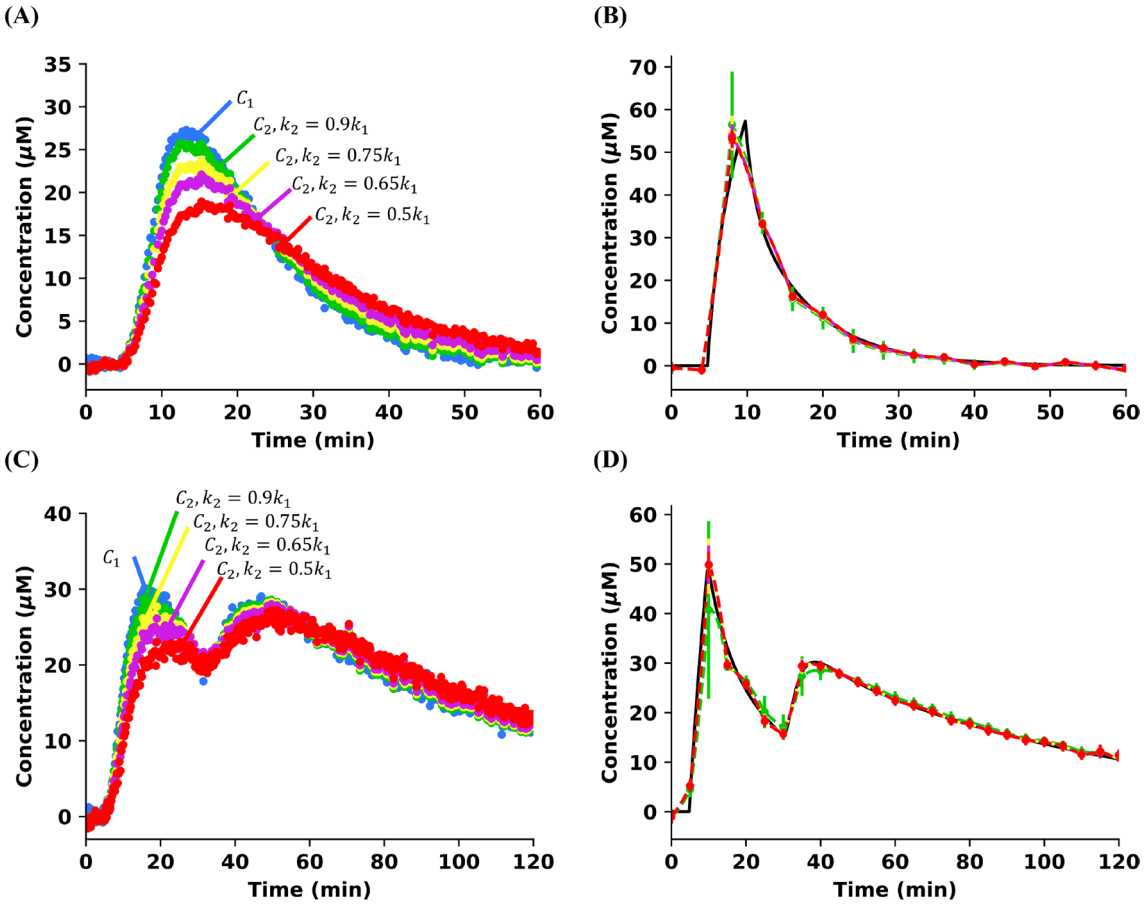

FIGURE 7 | Even when the difference between the two ISF measurement sites becomes small (i.e., the rate constants for diffusion to theme become close), we still retain the ability to estimate the plasma pharmacokinetics with clinically relevant accuracy. To demonstrate this, we employed the two plasma concentration–time courses described above: One when the plasma kinetics a single-compartment model (A, B), and another when the plasma concentration exhibits the effect of enterohepatic recirculation, a mechanism that generates particularly complex, nonmonotonic pharmacokinetic behavior (C, D). Using these two plasma time courses we then generated pairs of noisy ISF time courses using pairs of distribution rate constants that differ by as much as a factor of 2 or as little as 10% (A, C). Fitting these "measured" ISF time courses returns the original plasma drug profiles (solid black lines) to a clinically valuable but diminishing degree of accuracy even when the two distribution constants differ by as little as 10%. Our fits are shown by dots with 95% confidence intervals shown as solid lines with the colors matching the ratio between diffusion rates.

While assumed foreknowledge of the structure of the plasma pharmacokinetics (e.g., that it is described by a compartmental model of some order) improves the accuracy our plasma time course estimates from nonredundant ISF measurements, it is nevertheless possible to use such ISF measurements to estimate plasma time courses even without making such assumptions (Theorem 2). That is, it is possible to estimate plasma concentration–time courses from noisy ISF measurements even when the structure of the plasma pharmacokinetics is unknown or does not follow any particular model, an approach we have termed the "Minimum Assumptions Fit." Achieving this requires that, in addition to estimating $C_P(t)$, we also estimate the rate constants, k_1 and k_2, associated with the measurements, $C_1(t)$ and $C_2(t)$, collected at sites 1 and 2. A difficulty in doing so, however, is that, because they are related to the first derivatives of $C_1(t)$ and $C_2(t)$, the estimates of k_1 and k_2 are particularly sensitive to noise. To circumvent this, we have used a second order polynomial spline approach to "smooth" the noisy concentration measurements. This said, fitting a second order polynomial to every sampling interval would overfit the observations, rendering the estimation of rate constants and $C_P(t)$ impossible. To circumvent this requires selection of an appropriate time interval over which to smooth the observed data (by fitting the spline), which we performed using the Akaike Information Criterion (AIC), a common model selection criterion suitable for predictive models [28]. A limitation of this approach is that it constrains us to estimating only a few points of the plasma concentration, with the values in between being obtained by interpolation. Given the few-second resolution of subcutaneous EAB sensor measurements [9], however, this "down sampling" would be of little clinical consequence. For more details, see **Minimum Assumptions Fit** in **Methods**.

To explore the effectiveness of our Minimum Assumptions Fit approach, we employed two examples of known plasma pharmacokinetics, one exhibiting the same second order plasma pharmacokinetics (2PK) as our previous example, and a second following the enterohepatic reabsorption (EHR) model, as our test beds (Figure 6). The latter model is particularly challenging, as this class of pharmacokinetics produces significantly nonmonotonic plasma time courses [29]. Once again, we used simulations with distribution rate constants of $k_1 = 0.15$ min^{-1}

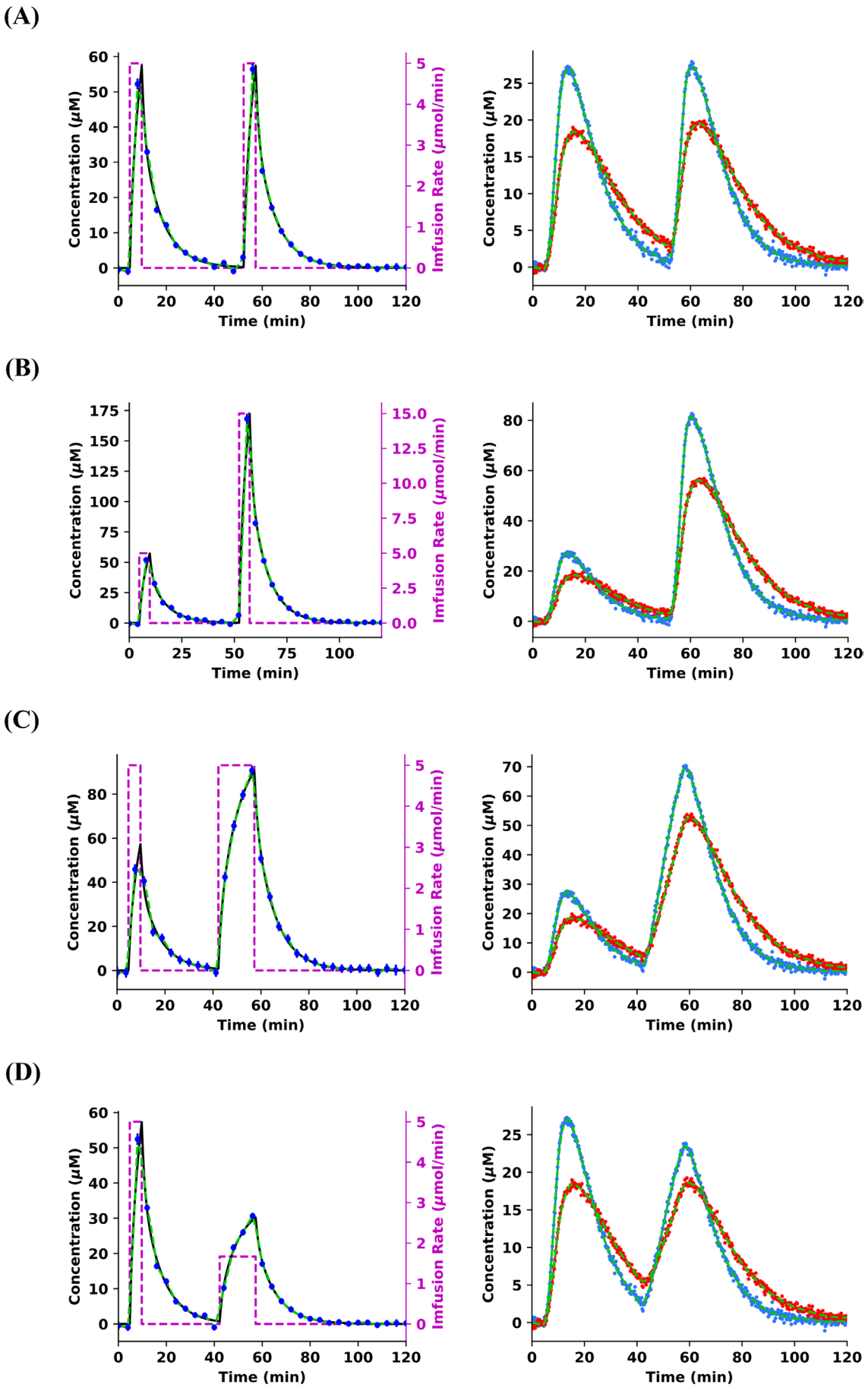

FIGURE 8 | Legend on next page.

FIGURE 8 | Our approach retains good accuracy irrespective of the exact drug infusion profile. For example, shown here are infusion profiles that include (A) two identical infusions, (B) two infusions of the same duration but different infusion rates, (C) the same infusion rate applied over two different infusion durations, (D) the same total drug amount infused over different durations. In these examples we employed a drug with second-order plasma pharmacokinetics and distribution rate constants differing by 50% ($k_1 = 0.15\ \text{min}^{-1}$ and $k_2 = 0.075\ \text{min}^{-1}$). In each example we recover the true plasma AUC with accuracies of better than 0.5% and C_{max} with accuracies of better than 10% except for the first C_{max} of the different diffusion duration case, for which the discrepancy is approximately 20%. For model and pharmacokinetic parameters, see Tables S1 and S2.

and $k_2 = 0.075\ \text{min}^{-1}$ and an experimentally justifiable noise at a signal-to-noise ratio of 30. The Minimum Assumptions Fit approach is able to accurately estimate plasma time courses under clinically plausible conditions without any prior knowledge of the structure of the plasma pharmacokinetics. To achieve this, our AIC-based procedure selected smoothing intervals of 4 min and 5 min for the 2PK and EHR examples, respectively, and thus estimates the plasma concentration with these time resolutions. The resulting estimated plasma concentration–time courses match the true plasma pharmacokinetics quite well. For example, the approach's estimates of C_{max}^{plasma}, which because it reflects a single, fleeting time point, is one of the more difficult parameters to estimate, are $53 \pm 2\,\mu\text{M}$ and $49 \pm 3\,\mu\text{M}$ (95% confidence intervals are calculated by using standard deviations derived analytically from solving the optimization problems) versus the "true" values of 57.3 μM and 49.8 μM for the 2PK and EHR cases, respectively (Figure 6).

Our ability to accurately estimate plasma concentration depends on the assumption that the measurement sites are nonredundant. That is, that the distribution rates k_1 and k_2 of each site differ by some appropriate degree. This, of course, raises the question of how strongly the accuracy of our estimated plasma time courses depends on the magnitude of this difference. To answer this, we next ran the Minimum Assumptions Fit procedure for data generated using distribution rate constants pairs differing by as much as 2-fold (as per our prior examples) or by as little as 10%, again keeping the signal-to-noise ratio of the ISF measurements fixed at the experimentally observed value of 30. Doing so, we find that, not surprisingly, as two distribution rates approach one another, the estimation of the plasma profiles become more uncertain (Figure 7). Nevertheless, we can retain clinically useful accuracy even when the two distribution rate constants are quite similar. For example, even when the distribution rates differ by as little as 10%, the estimated C_{max}^{plasma} which again, is the most difficult parameter to accurately estimate, are, at $57 \pm 12\,\mu\text{M}$ and $41 \pm 18\,\mu\text{M}$, reasonably tightly constrained on the true values of 57.3 and 49.8 μM for the 2PK and EHR examples, respectively.

Finally, our approach holds irrespective of the dosing regimen. To see this, we expanded our study of the 2PK example to include symmetric and asymmetric double infusions (Figure 8). In each case, our approach performed quite similarly to how it performed for the single-infusion examples presented above. Specifically, once again using distribution rates that differ by 50% ($k_1 = 0.15\ \text{min}^{-1}$ and $k_2 = 0.075\ \text{min}^{-1}$), we recover the true plasma AUC with accuracies better than 0.5% for all examples (see Table S2 for details).

We close by noting that the factors that define the rate constant for diffusion between the plasma and any given site in the ISF remain unknown, and thus the likelihood of observing rate constants at different sites in the ISF that differ is also unknown. That said, we hypothesize that attaching sensors to different regions of the body or sampling at different depths in or below the skin may achieve this due to site-specific differences in the degree of vascularization. We hope that the theoretical work we describe here will motivate experimental studies of this effect.

4 | Discussion

Here, we have shown that, under the assumptions that the drug in question is eliminated from the body via the plasma and not via the tissues that are under observation, the plasma and ISF are the only relevant compartments and that they communicate via passive diffusion, we can estimate plasma drug time courses with clinically acceptable accuracy using realistically noisy, highly time-resolved measurements performed in the ISF. Specifically, we find the following. (*i*) Provided that the time scale for distribution into the ISF is several-fold more rapid than the time scale over which plasma concentrations meaningfully change, ISF time courses closely parallel plasma time courses. (*ii*) For drugs for which this condition does not hold, plasma concentration–time courses can still be accurately estimated from measurements collected at a pair of ISF sites, provided the latter differ even slightly in the time scales with which the drug diffuses to them. Indeed, under the assumptions we have employed, we can estimate plasma concentration–time profiles with clinical accuracy even without a priori knowledge of the structure of the plasma time course and even when the distribution rate constants associated with the two ISF measurement sites differ by as little as 10%. Should this theoretical development hold true in clinical populations, the resulting ability to estimate plasma pharmacokinetics from minimally invasive subcutaneous or intradermal sensor placements has the potential to significantly improve the precision and reach of therapeutic drug monitoring and, with that, the safety and efficacy of drug delivery.

Author Contributions

All authors wrote the manuscript. K.W.P. designed the research. M.K.E. performed the research and analyzed the data. M.K.E. and J.P.H. contributed new analytical tools.

Conflicts of Interest

Murat K. Erdal is now employed by and Kevin W. Plaxco holds equity in Nutromics, a company that is commercializing in vivo drug sensors. All other authors declared no competing interests for this work. The main results and earlier versions of the figures were included in Murat K. Erdal's PhD dissertation.

References

1. H. C. Ates, J. A. Roberts, J. Lipman, A. E. G. Cass, G. A. Urban, and C. Dincer, "On-Site Therapeutic Drug Monitoring," *Trends in Biotechnology* 38, no. 11 (2020): 1262–1277, https://doi.org/10.1016/j.tibtech.2020.03.001.

2. B. D. Menz, S. L. Stocker, N. Verougstraete, et al., "Barriers and Opportunities for the Clinical Implementation of Therapeutic Drug Monitoring in Oncology," *British Journal of Clinical Pharmacology* 87, no. 2 (2021): 227–236, https://doi.org/10.1111/bcp.14372.

3. A. Abdulla, T. M. J. Ewoldt, N. G. M. Hunfeld, et al., "The Effect of Therapeutic Drug Monitoring of Beta-Lactam and Fluoroquinolones on Clinical Outcome in Critically Ill Patients: The DOLPHIN Trial Protocol of a Multi-Centre Randomised Controlled Trial," *BMC Infectious Diseases* 20, no. 1 (2020): 57, https://doi.org/10.1186/s12879-020-4781-x.

4. A. J. Fratoni, D. P. Nicolau, and J. L. Kuti, "A Guide to Therapeutic Drug Monitoring of β-Lactam Antibiotics," *Pharmacotheraphy Journal of Human Pharmacology and Drug Theraphy* 41, no. 2 (2021): 220–233, https://doi.org/10.1002/phar.2505.

5. M. J. Rybak, J. le, T. P. Lodise, et al., "Therapeutic Monitoring of Vancomycin for Serious Methicillin-Resistant *Staphylococcus aureus* Infections: A Revised Consensus Guideline and Review by the American Society of Health-System Pharmacists, the Infectious Diseases Society of America, the Pediatric Infectious Diseases Society, and the Society of Infectious Diseases Pharmacists," *Clinical Infectious Diseases* 71, no. 6 (2020): 1361–1364, https://doi.org/10.1093/cid/ciaa303.

6. N. Arroyo-Currás, J. Somerson, P. A. Vieira, K. L. Ploense, T. E. Kippin, and K. W. Plaxco, "Real-Time Measurement of Small Molecules Directly in Awake, Ambulatory Animals," *Proceedings of the National Academy of Sciences of the United States of America* 114, no. 4 (2017): 645–650, https://doi.org/10.1073/pnas.1613458114.

7. A. Chamorro-Garcia, J. Gerson, C. Flatebo, et al., "Real-Time, Seconds-Resolved Measurements of Plasma Methotrexate In Situ in the Living Body," *ACS Sensors* 8 (2022): 150–157, https://doi.org/10.1021/acssensors.2c01894.

8. P. Dauphin-Ducharme, K. Yang, N. Arroyo-Currás, et al., "Electrochemical Aptamer-Based Sensors for Improved Therapeutic Drug Monitoring and High-Precision, Feedback-Controlled Drug Delivery," *ACS Sensors* 4, no. 10 (2019): 2832–2837, https://doi.org/10.1021/acssensors.9b01616.

9. S. Lin, X. Cheng, J. Zhu, et al., "Wearable Microneedle-Based Electrochemical Aptamer Biosensing for Precision Dosing of Drugs With Narrow Therapeutic Windows," *Science Advances* 8, no. 38 (2022): eabq4539, https://doi.org/10.1126/sciadv.abq4539.

10. Y. Wu, F. Tehrani, H. Teymourian, et al., "Microneedle Aptamer-Based Sensors for Continuous, Real-Time Therapeutic Drug Monitoring," *Analytical Chemistry* 94, no. 23 (2022): 8335–8345, https://doi.org/10.1021/acs.analchem.2c00829.

11. N. Arroyo-Currás, G. Ortega, D. A. Copp, et al., "High-Precision Control of Plasma Drug Levels Using Feedback-Controlled Dosing," *ACS Pharmacology & Translational Science* 1, no. 2 (2018): 110–118, https://doi.org/10.1021/acsptsci.8b00033.

12. P. A. Vieira, C. B. Shin, N. Arroyo-Currás, et al., "Ultra-High-Precision, In-Vivo Pharmacokinetic Measurements Highlight the Need for and a Route Toward More Highly Personalized Medicine," *Frontiers in Molecular Biosciences* 6 (2019): 069, https://www.frontiersin.org/articles/10.3389/fmolb.2019.00069.

13. A. Idili, N. Arroyo-Currás, K. L. Ploense, et al., "Seconds-Resolved Pharmacokinetic Measurements of the Chemotherapeutic Irinotecan In Situ in the Living Body," *Chemical Science* 10, no. 35 (2019): 8164–8170, https://doi.org/10.1039/C9SC01495K.

14. A. Idili, J. Gerson, T. Kippin, and K. W. Plaxco, "Seconds-Resolved, In Situ Measurements of Plasma Phenylalanine Disposition Kinetics in Living Rats," *Analytical Chemistry* 93, no. 8 (2021): 4023–4032, https://doi.org/10.1021/acs.analchem.0c05024.

15. A. Z. Garza, S. B. Park, and R. Kocz, *Drug Elimination* (StatPearls Publishing, 2023), http://www.ncbi.nlm.nih.gov/books/NBK547662/.

16. A. Facchinetti, G. Sparacino, and C. Cobelli, "Reconstruction of Glucose in Plasma From Interstitial Fluid Continuous Glucose Monitoring Data: Role of Sensor Calibration," *Journal of Diabetes Science and Technology* 1, no. 5 (2007): 617–623, https://doi.org/10.1177/193229680700100504.

17. G. M. Steil, K. Rebrin, J. Mastrototaro, B. Bernaba, and M. F. Saad, "Determination of Plasma Glucose During Rapid Glucose Excursions With a Subcutaneous Glucose Sensor," *Diabetes Technology & Therapeutics* 5, no. 1 (2003): 27–31, https://doi.org/10.1089/152091503763816436.

18. E. Filippone, W. Kraft, and J. Farber, "The Nephrotoxicity of Vancomycin," *Clinical Pharmacology and Therapeutics* 102, no. 3 (2017): 459–469, https://doi.org/10.1002/cpt.726.

19. M. S. Ramirez and M. E. Tolmasky, "Aminoglycoside Modifying Enzymes," *Drug Resistance Updates* 13, no. 6 (2010): 151–171, https://doi.org/10.1016/j.drup.2010.08.003.

20. P. Macheras and A. Iliadis, *Modeling in Biopharmaceutics, Pharmacokinetics and Pharmacodynamics: Homogeneous and Heterogeneous Approaches*, vol. 30. Interdisciplinary Applied Mathematics (Springer International Publishing, 2016), https://doi.org/10.1007/978-3-319-27598-7.

21. J. P. Hespanha, *Linear Systems Theory*, Second ed. (Princeton University Press, 2018).

22. J. A. E. Andersson, J. Gillis, G. Horn, J. B. Rawlings, and M. Diehl, "CasADi: A Software Framework for Nonlinear Optimization and Optimal Control," *Mathematical Programming Computation* 11, no. 1 (2019): 1–36, https://doi.org/10.1007/s12532-018-0139-4.

23. A. Wächter and L. T. Biegler, "On the Implementation of an Interior-Point Filter Line-Search Algorithm for Large-Scale Nonlinear Programming," *Mathematical Programming* 106, no. 1 (2006): 25–57, https://doi.org/10.1007/s10107-004-0559-y.

24. A. A. Neath and J. E. Cavanaugh, "The Bayesian Information Criterion: Background, Derivation, and Applications," *WIREs Computational Statistics* 4, no. 2 (2012): 199–203, https://doi.org/10.1002/wics.199.

25. G. Schwarz, "Estimating the Dimension of a Model," *Annals of Statistics* 6, no. 2 (1978): 461–464.

26. E. Cengiz and W. V. Tamborlane, "A Tale of Two Compartments: Interstitial Versus Blood Glucose Monitoring," *Diabetes Technology & Therapeutics* 11, no. Suppl 1 (2009): S11–S16, https://doi.org/10.1089/dia.2009.0002.

27. J. Gerson, M. K. Erdal, P. Dauphin-Ducharme, et al., "A High-Precision View of Intercompartmental Drug Transport via Simultaneous, Seconds-Resolved, In Situ Measurements in the Vein and Brain," *British Journal of Pharmacology* 181, no. 20 (2024): 3869–3885, https://doi.org/10.1111/bph.16471.

28. J. Kuha, "AIC and BIC: Comparisons of Assumptions and Performance," *Sociological Methods & Research* 33, no. 2 (2004): 188–229, https://doi.org/10.1177/0049124103262065.

29. M. S. Roberts, B. M. Magnusson, F. J. Burczynski, and M. Weiss, "Enterohepatic Circulation: Physiological, Pharmacokinetic and Clinical Implications," *Clinical Pharmacokinetics* 41, no. 10 (2002): 751–790, https://doi.org/10.2165/00003088-200241100-00005.

Supporting Information

Additional supporting information can be found online in the Supporting Information section.